# Semiaromatic Polyamides with Enhanced Charge Carrier Mobility

Bilal Özen,[1] Nicolas Candau,[1] Cansel Temiz,[2] Ferdinand C. Grozema,[2] Grégory Stoclet,[3]
Christopher J.G. Plummer,[1] Holger Frauenrath[1,*]

[1] École Polytechnique Fédérale de Lausanne (EPFL)
Institute of Materials
Laboratory of Macromolecular and Organic Materials

EPFL–STI–IMX–LMOM
MXG 037, Station 12
1015 Lausanne, Switzerland

[2] Delft University of Technology
Department of Chemical Engineering

[3] Univ. Lille, CNRS, INRAE, Centrale Lille, UMR 8207 - UMET -
Unité Matériaux et Transformations, F-59000 Lille, France

* Corresponding Author:
holger.frauenrath@epfl.ch

## Abstract

The control of local order in polymer semiconductors using non-covalent interactions may be used to engineer materials with interesting combinations of mechanical and optoelectronic properties. To investigate the possibility of preparing n-type polymer semiconductors in which hydrogen bonding plays an important role in structural order and stability, we have used solution-phase polycondensation to incorporate dicyanoperylene bisimide repeat units into an aliphatic polyamide chain backbone. The morphology and thermomechanical characteristics of the resulting polyamides, in which the aliphatic spacer length was varied systematically, were comparable with those of existing semiaromatic engineering polyamides. At the same time, the charge carrier mobility as determined by pulse-radiolysis time-resolved microwave conductivity measurements was found to be about $10^{-2}$ $cm^2$ $V^{-1}$ $s^{-1}$, which is similar to that reported for low molecular weight perylene bisimides. Our results hence demonstrate that it is possible to use hydrogen bonding interactions as a means to introduce promising optoelectronic properties into high-performance engineering polymers.

## Introduction

Semiaromatic polyamides, particularly the polyphthalamides, are high-performance engineering thermoplastics because they exhibit outstanding thermomechanical property profiles,[1,2,3] but remain compatible with conventional industrial melt processing routes such as extrusion and injection moulding, in contrast to fully aromatic polyamides (polyaramids).[4–6] Although the development of semiaromatic polyamides and copolyamides has strongly focused on structural applications,[2,4,7] they also often show similar morphological features to recent high-performance polymer semiconductors, namely thin lamellar crystals and significant residual local order in the amorphous regions.[8–11] Semiaromatic polyamides whose repeat units contain π-conjugated segments may hence provide a promising route to engineering materials with novel combinations of optoelectronic and thermomechanical properties.

The widespread recognition of the importance of the morphology of semiconducting polymers at different length scales for their optoelectronic and thermomechanical properties[12,13] has led to a concerted effort to better understand their structure and property relationships, with emphasis on controlling the balance between short-range order and overall disorder.[14–16] Modification of the chain backbone with non-π-conjugated segments and side-chain engineering, in particular, have played a significant role in improving both the mechanical properties of π-conjugated polymers and device performance, through their influence on local order and hence the electronic coupling between neighboring chains.[17,18] A promising approach in this respect is the use of hydrogen bonding motifs that promote specific non-covalent intermolecular interactions.[19] Hydrogen bonding has been widely used to promote self-assembly of π-conjugated compounds into one-dimensional nanostructures in solution,[20–32] and to tailor the packing of π-conjugated compounds in the solid-state.[33,34] At the same time, it is well known to be key to the unique thermomechanical properties of engineering polyamides.[35] The introduction of hydrogen-bonded side chains into semiconducting polymers has consequently gained considerable recent attention. For instance, the presence of amide groups in the side chains of π-conjugated polymers based on diketopyrrolopyrrole [36,37] or isoindigo [38,39] repeat units has been found both to increase the strength of aggregation and crystallinity, resulting in enhanced charge carrier mobility and photovoltaic performance compared with the corresponding polymers with non-hydrogen-bonded side chains, and to enhance energy dissipation during mechanical deformation.[39,40]

By contrast, incorporation of hydrogen-bonded segments as non-conjugated spacers into semiconducting polymers has so far received limited attention. Bao et al. introduced a non-conjugated unit containing an amide group into the backbone of a π-conjugated polymer.[41] They found that 10 mol% of this co-monomer sufficed to alter the thin film morphology of the polymer network, leading to a reduction in elastic modulus and a moderate increase in the crack onset strain, but no significant changes in charge carrier properties. In another approach, the possibility of incorporating π-conjugated segments into a polyamide repeat unit was investigated by Mugurama et al., who prepared semiaromatic polyamides with oligothiophene units but provided no details of either their morphology, or their mechanical and optoelectronic properties.[42,43] We recently reported semicrystalline semiaromatic polyamides with bithiophene units and demonstrated that such materials indeed combined the thermomechanical characteristics of typical semiaromatic engineering polyamides with significant charge carrier mobility.[44]

Here, we report the first example of polyamides containing electron deficient, n-type semiconducting dicyanoperylene bisimide repeat units. Four such polyamides with different aliphatic spacer lengths were found to show not only good thermal stability and shear moduli in the range 0.75–0.93 GPa, but also H-type coupling of the dicyanoperylene bisimide chromophores in the solid-state, and charge carrier mobilities of about 0.01 $cm^2V^{-1}s^{-1}$. The dicyanoperylene bisimide-containing polyamides thus combined the thermomechanical properties of typical engineering polyamides with optoelectronic properties typical of organic and polymer semiconductors.

## Experimental Part

*Materials and Instrumentation*

*Materials.* All materials and solvents for reactions were purchased from commercial suppliers and used without further purification. Chlorendic hydroxylimide[45] and 1,7-dibromoperylene-3,4:9,10-tetracarboxylic dianhydride **2** were prepared following a literature procedure.[46] Chromatography solvents were purchased as reagent grade and distilled once prior to use. The progress of the reactions was monitored by thin-layer chromatography (TLC) on Merck TLC plates (Silica gel 60 $F_{254}$) using DCM/EtOAc as the eluent. UV light (254 nm) was used for detection of compounds on the TLC plates. Silica gel (Geduran Si 60 Merck, 40-60 um) was used for column chromatography.

*NMR Spectroscopy.* NMR spectroscopy was carried out at 298 K with Bruker Avance III 400 or 600 spectrometers at frequencies of 400 MHz, 600 MHz for $^{1}$H nuclei, and 100 MHz, 150 MHz for $^{13}$C nuclei, respectively. The spectra were calibrated using the residual solvent peaks of $CD_2Cl_2$ (5.32 ppm $^{1}$H NMR; 53.84 ppm $^{13}$C NMR) or $CDCl_3$ (7.26 ppm $^{1}$H NMR; 77.16 ppm $^{13}$C NMR). The $^{1}$H NMR spectrum of 1,7-dibromoperylene-3,4:9,10-tetracarboxylic dianhydride **2** was recorded in conc. $D_2SO_4$ (96–98% in $D_2O$) with 4,4-dimethyl-4-silapentane-1-sulfonic acid (DSS) as an internal refence material. The $^{1}$H NMR spectra of the polyamides were recorded in TFA-*d* / $CDCl_3$ (1:3) mixtures.

*Infrared Spectroscopy.* Infrared spectra were measured on a JASCO FT/IR 6300 spectrometer using the Miracle attenuated total reflection (ATR) accessory from PIKE.

*Optical Spectroscopy.* UV-vis spectra were measured with a Jasco V-670 spectrometer. Solution-phase spectra of trifluoroacetic acid (TFA) solutions (0.1 mg/mL) were obtained using Hellma quartz cuvettes (1 cm path length), and thin film spectra were measured from specimens spin-coated onto a quartz substrate (4000 rpm, 1 min) from 100 µL of a stock solution (1 mg/mL). Solution-phase fluorescence spectra were obtained with a Jasco FP-6500 spectrofluorometer from TFA solutions (0.01 mg/mL) using Hellma quartz cuvettes (1 × 1 cm$^2$) at an excitation wavelength of 527 nm. Solid-state fluorescence spectroscopy made use of films obtained from dispersions prepared by stirring 5 mg of the compounds in 5.2 g of a 17% *w/v* solution of PMMA in toluene. These dispersions were spin-coated (4000 rpm, 1 min) onto transparent polyester substrates (Byko-Charts, BYK Gardner, USA), and the resulting films were first dried in air for 2 h and then in high vacuum for a week after removal of the substrate. The fluorescence spectra of these films were recorded with a Horiba Jobin FluoroMax-3.

*Mass Spectrometry.* High-resolution mass spectrometry was carried out with a Waters QTOF Xevo G2-S for APPI.

*Gel Permeation Chromatography (GPC).* The number and weight average molecular weights, $M_n$ and $M_w$, and the dispersities, $Đ$, of the polyamides were determined using an Agilent 1260 Infinity GPC/SEC system with a refractive index detector and a total column length of 650 mm (PSS PFG, 100 Å). 1,1,1,3,3,3-hexafluoropropane-2-ol (HFIP) was used as the eluent at a flow rate of 1 mL/min and a temperature of 25 °C. Six poly(methyl methacrylate) (PMMA) standards with molar masses between 2'000 and 44'000 g/mol and $Đ \leq 1.1$ were used for calibration. The derivatized polyamides and PMMA standards were all dissolved in neat HFIP ($c$ = 3 mg/mL).

*Thermal Characterization.* Thermogravimetric analyses (TGA) were conducted with a Perkin Elmer TGA 4000. Samples of 5–10 mg were dried in high vacuum at 80 °C for 24 h and then heated from 30 °C to 950 °C at a scanning rate of 10 °C/min under nitrogen flow (20 mL/min). Differential scanning calorimetry (DSC) was carried out with a Mettler Toledo, DSC $3^+$ STAR$^e$ System calorimeter at a scanning rate of 10°C/min under nitrogen flow (50 mL/min). Specimens of about 3–5 mg were first heated to a 220 °C and then cooled to 0 °C at a cooling rate of 10 °C/min in order to erase the effects of their thermal history.

*Small-Angle X-Ray Scattering and Wide-Angle X-Ray Diffraction (SAXS / WAXD).* 2D SAXS and WAXD measurements were performed with a Xeuss 2.0 apparatus (Xenocs) equipped with a micro source (CuKα radiation, λ = 1.54 Å) and point collimation. The sample-to-detector distance, which was around 18 cm for WAXD and 150 cm for SAXS, was calibrated using silver behenate as a standard. The data were recorded in transmission mode with a beam size of $500 \times 500\ \mu m^2$ and a 2D Pilatus 200K detector. Standard corrections were applied to the WAXD and SAXS patterns before their analysis. The intensity profiles were obtained by azimuthal integration of the 2D patterns using the fit2D software. Trial crystal structures for the polyamides with perylene bisimide units were generated using the BIOVIA Materials Studio graphics user interface. Their geometry was then optimized with respect to all structural degrees of freedom subject to periodic boundary conditions, using classical force field-based energy minimization with the generic Dreiding force field[47] and the method of steepest descents with charge equilibration. WAXD patterns were simulated using the BIOVIA Reflex software package.

*Dynamic Mechanical Analysis.* Dynamic mechanical testing (861$^e$, Mettler Toledo) was performed in shear mode at room temperature with a strain amplitude of 0.1%. Each specimen was tested at successive frequencies of 10, 1 and 0.1 Hz. The test specimens were compressed into 5 mm diameter cylindrical pellets with heights of 0.30–0.60 mm.

*Pulse Radiolysis Time-Resolved Microwave Conductivity.* Charges were generated in powder samples (20–50 mg) by irradiation with short pulses (2–20 ns) of high-energy electrons (3 MeV) from a Van de Graaff accelerator. The penetration depth of these high-energy electrons in the materials is several millimeters, resulting in close to homogenous ionization and hence a uniform concentration of charges. The change in conductivity of the material due to charges generated by the irradiation, was probed using high frequency microwaves (28 to 38 GHz). The fractional change in the microwave

power ($\Delta P/P$) absorbed on irradiation is directly proportional to the change in the conductivity ($\Delta\sigma$) according to

$$\frac{\Delta P}{P} = -A\Delta\sigma$$

where the sensitivity factor, $A$, is a sensitivity factor that depends on the geometric and dielectric properties of the material.[48] The conductivity ($\Delta\sigma$) is related to the mobility of all charged species, and their concentration, $N_p$, through

$$\Delta\sigma = eN_p \sum \mu$$

where $e$ is the elementary charge ($1.6 \times 10^{-19}$ C). This this is equation allows the mobility of the charge carriers to be calculated given a reasonable estimate of their concentration. Such an estimate may be obtained from dosimetry measurements, which provides the amount of energy deposited by the electron pulse, as described in detail previously.[49]

*Synthetic Procedures and Analytical Data*

**1,7-Dibromoperylene-3,4:9,10-tetracarboxylic dianhydride (2).** Perylene-3,4:9,10-tetracarboxylic acid bisanhydride (20 g, 51 mmol) was suspended in concentrated $H_2SO_4$ (300 mL). This mixture was stirred for 16 h at room temperature before powdered iodine (0.52 g, 2.05 mmol) was added. It was then heated to 85 °C, and bromine (5.8 mL, 112 mmol, 2.2 equiv.) added dropwise over 6 h. On completion of the addition, the reaction mixture was heated for a further 48 h and then allowed to cool to room temperature. The excess bromine was removed with a gentle stream of argon and reduced by bubbling the stream through a saturated $Na_2S_2O_3$ solution. After cooling to 0 °C, 100 mL of deionized water was carefully added. Filtration of the resulting precipitate and washing with concentrated $H_2SO_4$ (50 mL) and deionized water (2 L) yielded a red solid powder, comprising a mixture of 1,7-dibromo, 1,6-dibromo and 1,7,6-tribromoperylene bisimide in a ratio of 75:17:8, as revealed by $^1$H NMR in conc. $D_2SO_4$ (96–98% in $D_2O$) (Supplementary Figure S1). This mixture was used without further purification in the next step (26.4 g, 97%). HRMS (APPI): calcd for $C_{24}H_6Br_2O_6$: 547.8537 $[M]^-$; found: 547.8519.

**1,7-Dibromoperylene-3,4:9,10-tetracarboximide-*N,N'*-di(butanoic acid) di(*tert*-butyl ester) (3).** Compound **2** (13 g, 23.6 mmol), 4-aminobutyric acid *tert*-butyl ester hydrochloride (19 g, 97.1 mmol) and $Zn(OAc)_2$ (4.3 g, 23.6 mmol) were suspended in freshly distilled quinoline (350 mL) in an argon flow. The reaction mixture was heated to 100 °C for 16 h and then cooled to room temperature prior

to solvent removal in vacuum. The resulting residue was redissolved in DCM (2 L), washed twice with 1 M HCl twice and once with brine, and finally dried over $MgSO_4$. After solvent removal, the crude product was purified by column chromatography (silica gel, 5% EtOAc in DCM) to give **3** as a mixture of the 1,7-dibromo and the 1,6-dibromo regioisomers (75:25) as a dark red powder (15.5 g, 79% yield). $^1$H NMR (400 MHz, $CDCl_3$): $\delta$ = 9.50 (d, $J$ = 8.2 Hz, 2H), 8.94 (s, 2H), 8.72 (d, $J$ = 8.1 Hz, 2H), 4.28 (t, $J$ = 7.2 Hz, 4H), 2.39 (t, $J$ = 7.4 Hz, 4H), 2.19–1.90 (m, 4H), 1.44 (s, 18H) ppm. $^{13}$C NMR (101 MHz, $CDCl_3$, **[m,n]** stands for the corresponding isomer): $\delta$ = 172.19, 163.21 **[1,6]**, 162.83 **[1,7]**, 162.33 **[1,7]**, 161.97 **[1,6]**, 138.13 **[1,6]**, 138.04 **[1,7]**, 133.09 **[1,6]**, 132.84 **[1,7]**, 132.71 **[1,7]**, 132.29 **[1,6]**, 130.02 **[1,7]**, 129.90 **[1,6]**, 129.10 **[1,7]**, 128.46 **[1,7]**, 128.10 **[1,6]**, 127.87 **[1,6]**, 127.70 **[1,6]**, 126.89 **[1,7]**, 126.06 **[1,6]**, 123.28 **[1,6]**, 123.09 **[1,7]**, 122.65 **[1,7]**, 122.35 **[1,6]**, 121.70 **[1,6]**, 120.90 **[1,7]**, 80.53, 40.13, 33.27, 28.21, 23.59 ppm. HRMS (APPI): calcd for $C_{40}H_{36}Br_2N_2O_8$: 830.0833 [$M$]$^+$; found: 830.0819. $R_f$ : 0.34 (5% EtOAc in DCM).

**1,7-Dicyanoperylene-3,4:9,10-tetracarboximide-*N,N*'-di(butanoic acid) di(*tert*-butyl ester) (4).** Compound **3** (13.5 g, 15.95 mmol), $Zn(CN)_2$ (15.9 g, 135.55 mmol), tris(dibenzylideneacetone)-dipalladium(0) ($Pd_2(dba)_3$) (3.65 g, 4 mmol) and 1,1'-bis(diphenylphosphino)-ferrocene (dppf) (2.21 g, 4 mmol), were suspended in dry dioxane (1 L) in an argon atmosphere. The dark-orange suspension was heated to 95 °C for 48 h and then cooled to room temperature. The amount of solvent was reduced to about one third in vacuum, before diluting the solution with DCM (600 mL) and filtering over celite. After solvent removal, the crude product was suspended in EtOAc, filtered, and purified by column chromatography (silica gel, 7% EtOAc in DCM) to give **4** as a mixture of the 1,7-dibromo and the 1,6-dibromo regioisomers (75:25) as a red solid powder (4.6 g, 40%). $^1$H NMR (400 MHz, TFA-*d*:$CD_2Cl_2$= 1:3, **[m,n]** stands for the corresponding isomer): $\delta$ = 9.79–9.68 (m, **[1,6]** and **[1,7]**, 2H), 9.18 (s, **[1,6]**, 2H), 9.13 (s, **[1,7]**, 2H), 9.04 (d, **[1,7]**, $J$ = 8.2 Hz, 2H), 8.98 (d, **[1,6]**, $J$ = 8.2 Hz, 2H), 4.41 (t, $J$ = 7.1 Hz, 4H), 2.69 (t, $J$ = 7.3 Hz, 4H), 2.22 (m, 4H), 1.59 (s, 18H) ppm. $^{13}$C NMR (101 MHz, TFA-*d*:$CD_2Cl_2$= 1:3): $\delta$ = 181.30, 165.13 **[1,6]**, 164.60 **[1,7]**, 163.92 **[1,7]**, 163.40 **[1,6]**, 140.07 **[1,6]**, 139.75 **[1,6]**, 138.17 **[1,7]**, 137.84, **[1,7]**, 135.45 **[1,7]**, 133.66 **[1,7]**, 133.26 **[1,6]**, 132.00 **[1,6]**, 130.54 **[1,7]**, 130.34 **[1,7]**, 129.06 **[1,6]**, 128.29 **[1,6]**, 127.71 **[1,7]**, 127.09 **[1,6]**, 125.87 **[1,6]**, 124.96 **[1,7]**, 123.99 **[1,7]**, 123.19 **[1,6]**, 118.99 **[1,7]**, 109.46 **[1,6]**, 109.10 **[1,7]**, 89.72, 41.32, 31.94, 27.84, 23.33 ppm. HRMS (APPI): calcd for $C_{42}H_{36}N_4O_8$: 724.2528 [$M$]$^+$; found: 724.2528. $R_f$ : 0.38 (7% EtOAc in DCM).

**1,7-Dicyanoperylene-3,4:9,10-tetracarboximide-*N,N'*-di(butanoic acid) (5).** Compound **4** (1.6 g, 2.2 mmol) was suspended in 180 mL $CHCl_3$ before addition of TFA (96 mL, 1.2 mol). The mixture was heated to reflux and stirred for 15 h. It was then cooled to room temperature, and the volatiles removed under vacuum. The crude product was suspended in 1 M HCl (300 mL) and ultrasonicated for 20 min. Filtration and subsequent drying of the resulting precipitate yielded **5** as a mixture of the 1,7-dibromo and the 1,6-dibromo regioisomers (75:25) as a red solid powder (1.3 g, 96%), which was used without further purification in the next step. $^1$H NMR (400 MHz, TFA-*d*:$CD_2Cl_2$= 1:3, **[m,n]** stands for the corresponding isomer): $\delta$ = 9.78–9.74 (m, **[1,6]** and **[1,7]**, 2H), 9.22 (s, **[1,6]**, 2H), 9.17 (s, **[1,7]**, 2H), 9.08 (d, **[1,7]**, $J$ = 8.2 Hz, 2H), 9.01 (d, **[1,6]**, $J$ = 8.2 Hz, 2H), 4.44 (t, $J$ = 7.0 Hz, 4H), 2.71 (t, $J$ = 7.1 Hz, 4H), 2.30–2.20 (m, 4H) ppm. $^{13}$C NMR (101 MHz, TFA-*d*:$CD_2Cl_2$= 1:3): $\delta$ = 180.54, 165.54 **[1,6]**, 165.00 **[1,7]**, 164.32 **[1,7]**, 163.79 **[1,6]**, 140.48 **[1,6]**, 140.08 **[1,6]**, 138.54 **[1,7]**, 138.14, **[1,7]**, 135.81 **[1,7]**, 133.92 **[1,7]**, 133.58 **[1,6]**, 132.24 **[1,6]**, 130.80 **[1,7]**, 130.62 **[1,7]**, 129.28 **[1,6]**, 128.51 **[1,6]**, 127.92 **[1,7]**, 127.28 **[1,6]**, 126.07 **[1,6]**, 125.15 **[1,7]**, 124.17 **[1,7]**, 123.37 **[1,6]**, 118.98 **[1,7]**, 109.57 **[1,6]**, 109.20 **[1,7]**, 40.53, 31.02, 22.42 ppm. HRMS (APPI): calcd for $C_{34}H_{20}N_4O_8$: 612.1287 ([*M*]$^-$); found: 612.1271.

**1,7-Dicyanoperylene-3,4:9,10-tetracarboximide-*N,N'*- bis (*N*-propylbutanamide) (6).** Compound **5** (100 mg, 0.16 mmol) was suspended in dry DMF (10 mL) in a flame-dried 50 mL Schlenk tube prior to the addition of chlorendic hydroxylimide (132 mg, 0.34 mmol) and *N,N'*-diisopropylcarbodiimide (DIC) (0.17 mL, 1.1 mmol, 6.5 equiv.) in an argon atmosphere. The reaction mixture was heated to 50 °C for 14 h. The volatiles were then removed in vacuum, and the residue was dissolved in dry THF (20 mL). Propylamine (0.27 mL, 3.3 mmol, 20 equiv.) was then added, and the reaction mixture was heated to 50 °C for 14 h. After removal of the volatiles, the crude product was suspended in MeOH. Filtration and subsequent washing with MeOH yielded **6** as a mixture of the 1,7-dibromo and the 1,6-dibromo regioisomers (75:25) as a dark red solid powder (95 mg, 84%). $^1$H NMR (800 MHz, TFA-*d*, **[m,n]** stands for corresponding isomer): $\delta$ = 9.94 (d, **[1,6]**, $J$ = 8.6 Hz, 2H), 9.93 (d, **[1,7]**, $J$ = 8.2 Hz, 2H), 9.37 (s, **[1,6]**, 2H), 9.32 (s, **[1,7]**, 2H), 9.24 (d, **[1,7]**, $J$ = 8.1 Hz, 2H), 9.17 (d, **[1,6]**, $J$ = 8.1 Hz, 2H), 4.60 (h, $J$ = 7.6, 7.1 Hz, 4H), 3.74 (q, $J$ = 8.0, 7.5 Hz, 4H), 3.06 (t, $J$ = 7.3 Hz, 4H), 2.52 (p, $J$ = 6.6 Hz, 4H), 1.93 (h, $J$ = 7.2 Hz, 4H), 1.19 (t, $J$ = 7.5 Hz, 6H) ppm. $^{13}$C NMR (201 MHz, TFA-*d*): $\delta$ = 178.55, 165.73 **[1,6]**, 165.18 **[1,7]**, 164.47 **[1,7]**, 163.94 **[1,6]**, 140.35**[1,6]**, 139.61 **[1,6]**, 138.44 **[1,7]**, 137.65 **[1,7]**, 135.47 **[1,7]**, 133.62 **[1,7]**, 133.19 **[1,6]**, 132.00 **[1,6]**, 131.92 **[1,6]**, 130.35 **[1,7]**, 130.13 **[1,7]**, 128.75 **[1,6]**, 127.95 **[1,6]**, 127.33 **[1,7]**, 126.66 **[1,6]**, 125.12 **[1,6]**, 124.30 **[1,7]**, 123.32 **[1,7]**, 122.63 **[1,6]**, 117.68

**[1,6]**, 117.12 **[1,7]**, 108.86 **[1,6]**, 108.45 **[1,7]**, 45.13, 40.17, 30.96, 24.29, 21.18, 9.68 ppm. HRMS (APPI): calcd for $C_{40}H_{35}N_6O_6$: 695.2613 ([*M*+H]$^+$); found: 695.2603.

*General Procedure for the Synthesis of Dicyanoperylene Bisimide-Containing Polyamides (PAnPBICN2)*. Compound **5** (250 mg, 0.41 mmol) was suspended in dry DMF (25 mL) in a flame-dried 50 mL Schlenk tube before the addition of chlorendic hydroxylimide (331 mg, 0.86 mmol) and *N,N'*-diisopropylcarbodiimide (DIC) (0.38 mL, 2.5 mmol, 6 equiv.) in an argon atmosphere. The reaction mixture was heated to 50 °C for 14 h. The volatiles were removed in vacuum, and the residue was dissolved in dry DMSO (10 mL). The aliphatic diamine (1 equiv.) was then added, and the reaction mixture was heated to 120 °C under vigorous stirring. After 48 h, the solution was poured into MeOH (250 mL), and the resulting slurry was stirred for 15 min. The precipitate was filtered off, washed several times with hot MeOH and dried in vacuum to yield the desired polyamide as dark red powder.

*General Procedure for the Derivatization of Dicyanoperylene Bisimide-Containing Polyamides (PAnPBICN2)*. For molecular weight determination by GPC, the polyamides were derivatized as follows. The polyamide **PA*n*PBICN2** (20 mg) was suspended in dry DCM (3 mL) in a flame-dried 10 mL Schlenk tube before the addition of trifluoroacetic anhydride (TFAA) (0.8 mL, 5.75 mmol) in an argon atmosphere. The reaction mixture was stirred at room temperature for 48 h and the derivatized polyamides, i.e., the corresponding poly(trifluoroacetylimide)s, were obtained by gently evaporating the volatiles at 40 °C. The polymers were soluble in HFIP ($c$ = 3 mg/mL).

**Poly(hexamethylene dicyanoperylene bisimide *N,N'*-dibutanamide) (PA6PBICN2).** The general procedure for the synthesis of dicyanoperylene bisimide-containing polyamides was followed, starting from **5** (250 mg, 0.41 mmol), chlorendic hydroxylimide (331 mg, 0.86 mmol), *N,N'*-diisopropylcarbodiimide (DIC) (0.38 mL, 2.5 mmol, 6 equiv.), and 1,6-hexanediamine (47 mg, 0.41 mmol), to give the desired polyamide **PA6PBICN2** in a yield of 240 mg (85%) after precipitation. $^1$H NMR (400 MHz, TFA-*d*:$CDCl_3$= 1:3): $\delta$ = 9.88–9.77 (m, 2H), 9.30–9.20 (m, 2H), 9.20–9.01 (m, 2H), 4.51 (br, 4H), 3.70 (br, 4H), 2.96 (br, 4H), 2.43 (br, 4H), 1.87 (br, 4H), 1.59 (br, 4H) ppm. GPC (HFIP): $M_n$ = 9'700 ($Đ$ = 2.0).

**Poly(octamethylene dicyanoperylene bisimide *N,N'*-dibutanamide) (PA8PBICN2).** The general procedure for the synthesis of dicyanoperylene bisimide-containing polyamides was followed, starting from **5** (250 mg, 0.41 mmol), chlorendic hydroxylimide (331 mg, 0.86 mmol), *N,N'*-diisopropylcarbodiimide (DIC) (0.38 mL, 2.5 mmol, 6 equiv.), and 1,8-octanediamine (58.85 mg,

0.41 mmol), to give the desired polyamide **PA8PBICN2** in a yield of 272 mg (92%) after precipitation. $^1$H NMR (400 MHz, TFA-*d*:$CDCl_3$= 1:3): $\delta$ = 9.92–9.72 (m, 2H), 9.30–9.20 (m, 2H), 9.20–9.05 (m, 2H), 4.51 (br, 4H), 3.69 (br, 4H), 2.96 (br, 4H), 2.43 (br, 4H), 1.85 (br, 2H), 1.51 (br, 8H) ppm. GPC (HFIP): $M_n$ = 11'100 ($Đ$ = 1.9).

**Poly(decamethylene dicyanoperylene bisimide *N,N'*-dibutanamide) (PA10PBICN2).** The general procedure for the synthesis of dicyanoperylene bisimide-containing polyamides was followed, starting from **5** (250 mg, 0.41 mmol), chlorendic hydroxylimide (331 mg, 0.86 mmol), *N,N'*-diisopropylcarbodiimide (DIC) (0.38 mL, 2.5 mmol, 6 equiv.), and 1,10-decanediamine (70.3 mg, 0.41 mmol), to give the desired polyamide **PA10PBICN2** in a yield of 280 mg (92%) after precipitation. $^1$H NMR (400 MHz, TFA-*d*:$CDCl_3$= 1:3): $\delta$ = 9.88–9.82 (m, 2H), 9.30–9.20 (m, 2H), 9.20–9.06 (m, 2H), 4.52 (br, 4H), 3.70 (br, 4H), 2.98 (br, 4H), 2.44 (br, 4H), 1.94–1.78 (m, 4H), 1.47 (m, 12H) ppm. GPC (HFIP): $M_n$ = 9'400 ($Đ$ = 2).

**Poly(dodecamethylene dicyanoperylene bisimide *N,N'*-dibutanamide) (PA12PBICN2).** The general procedure for the synthesis of dicyanoperylene bisimide-containing polyamides, was followed starting from **5** (250 mg, 0.41 mmol), chlorendic hydroxylimide (331 mg, 0.86 mmol), *N,N'*-diisopropylcarbodiimide (DIC) (0.38 mL, 2.5 mmol, 6 equiv.), and 1,12-dodecanediamine (81.7 mg, 0.41 mmol), to give the desired polyamide **PA12PBICN2** in a yield of 270 mg (85%) after precipitation. $^1$H NMR (400 MHz, TFA-*d*:$CDCl_3$= 1:3): $\delta$ = 9.92–9.82 (m, 2H), 9.30–9.20 (m, 2H), 9.20–9.05 (m, 2H), 4.51 (br, 4H), 3.69 (t, $J$ = 7.2 Hz, 4H), 2.97 (br, 4H), 2.43 (m, 4H), 1.83 (br, 4H), 1.44 (m, 4H) ppm. GPC (HFIP): $M_n$ = 15'500 ($Đ$ = 2.0).

## Results and Discussion

*Synthesis and Characterization of Dicyanoperylene Bisimide-Containing Semiaromatic Polyamides*

The synthesis of dicyanoperylene bisimide dibutyric acid **5** was performed in four steps starting from commercially available perylene bisanhydride (Scheme 1). Following a published procedure,[46] the bromination of perylene bisanhydride was carried out by electrophilic substitution with bromine, using iodine as a Lewis catalyst. The insolubility of the crude product prohibited further purification, resulting in a mixture of non-separable 1,7-dibromo, 1,6-dibromo, and 1,7,6-tribromoperylene bisimides **2** in a ratio of 75:17:8 in a yield of 97% (26 g) (Supplementary Figure S1). The butyl spacer between the chromophore and ester functionality was introduced by subsequent imidization of the

regioisomeric mixture with 4-aminobutyric acid *tert*-butyl ester hydrochloride to give di(*tert*-butyl ester) **3** after purification with column chromatography in a yield of 79% (15.5 g), as a mixture of the desired 1,7-dibromo and the 1,6-dibromo regioisomers in a ratio of 75:25, which also remained inseparable in the subsequent synthetic steps. The corresponding dicyanoperylene bisimide dibutanoate **4** was prepared by a Pd-catalyzed cyanation of compound **3** with $Zn(OAc)_2$, 1,1'-bis(diphenylphosphino)-ferrocene (dppf) and tris(dibenzylideneacetone)-dipalladium(0) ($Pd_2(dba)_3$) in dry dioxane at 95 °C for 2 d. After suspension in EtOAc and filtration, purification by column chromatography gave compound **4** as a red solid powder in a yield of 40% (4.6 g). Subsequent deprotection of the *tert*-butyl esters with TFA gave dicyanoperylene bisimide dibutanoic acid **5** in almost quantitative yield (1.3 g).

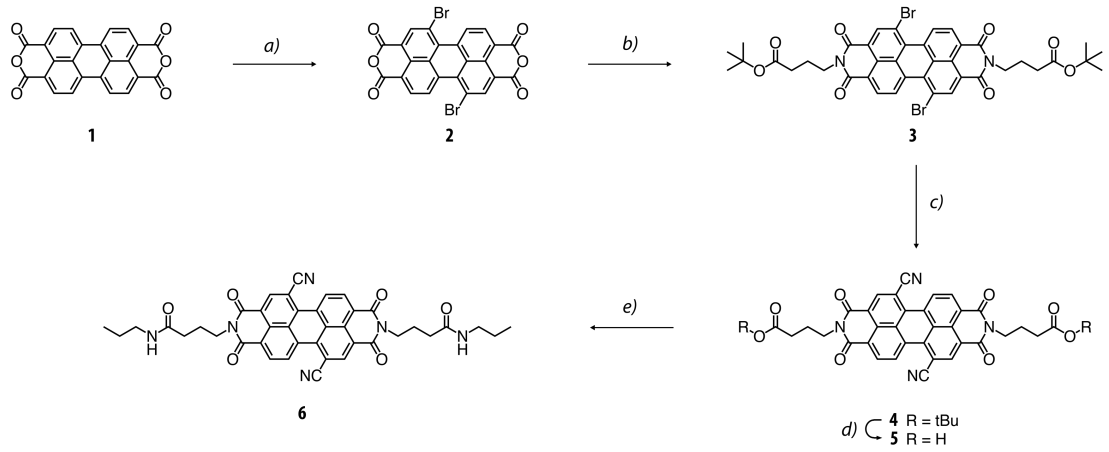


**Scheme 1.** Synthesis of the dicyanoperylene bisimide *N,N'*-dibutanoic acid **5** and the corresponding diamide model compound **6**. *Reagents and conditions: a)* $Br_2$, cat. amount of $I_2$, conc. $H_2SO_4$ (96%), 85 °C, 3 d, 97% yield; *b)* 4-aminobutyric acid *tert*-butyl ester hydrochloride, $Zn(OAc)_2$, quinoline, 100 °C, 16 h, 79% yield; *c)* $Zn(CN)_2$, $Pd_2(dba)_3$, dppf, dioxane, 95 °C, 48 h, 40% yield; *d)* $CHCl_3$, TFA, reflux, 15 h, 96% yield; *e)* chlorendic hydroxylimide, DIC, propylamine, DMF/THF, 50 °C, 28 h, 84% yield.

Because of solubility issues encountered with **5**, the Yamazaki-Higashi solution-phase polycondensation route[50,51] was not an option and an alternative procedure was therefore used. The carbodiimide-promoted reaction of compound **5** with chlorendic hydroxylimide resulted in the corresponding active ester monomer, which was used *in situ* for the synthesis of the dicyanoperylene bisimide-containing polyamides **PA*n*PBICN2** (*n* = 6, 8, 10, 12) by solution-phase polycondensation with 1,6-hexanediamine, 1,8-octanediamine, 1,10-decanediamine, and 1,12-dodecanediamine, respectively, in yields of 85–92% (240–280 mg) after precipitation (Scheme 2, Table 1). Likewise, the *in situ* activation of dibutanoic acid **5** with chlorendic hydroxylimide followed by coupling to

propylamine gave the diamide model compound **6** in a yield of 84% (95 mg). The continued presence of the 1,6-dicyano regioisomer was shown by 2D NMR spectroscopy (Supplementary Figure S2).

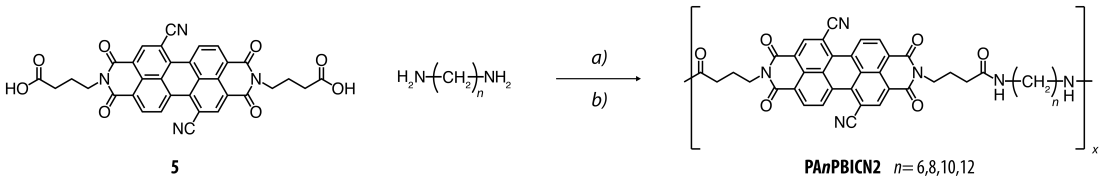


**Scheme 2.** Synthesis of dicyanoperylene bisimide -containing polyamides **PA*n*PBICN2**. *Reagents and conditions: a)* Chlorendic hydroxylimide, DIC, DMF, 50 °C, 14 h, *b)* DMSO, 120 °C, 2 d, 85–92%.

All polyamides were soluble in trifluoroacetic acid (TFA) and *m*-cresol at room temperature, but remained insoluble in most common polar aprotic solvents, including dimethyl sulfoxide (DMSO), dimethylformamide (DMF), *N*-metyl-2-pyrrolidone (NMP), hexamethylphosphoramide (HMPA), *o*-dichlorobenzene, cyclohexanone, or dimethylacetamide, as well as quinoline, glacial acetic acid, 1,1,1,3,3,3-hexa-fluoropropan-2-ol (HFIP), *o*-/*m*-xylene or chlorobenzene, even at elevated temperatures.

**Table 1.** Yields, number and weight-average molecular weights ($M_n$, $M_w$), and dispersities ($Đ$) obtained from gel permeation chromatography of the dicyanoperylene bisimide-containing polyamides **PA*n*PBICN2**.

| **Polyamide** | | | | GPC | | |
|---|---|---|---|---|---|---|
| **PA*n*PBICN2** | *n* | Amount [mg] | Yield [%] | $M_n$ [g/mol] | $M_w$ [g/mol] | $Đ$ |
| **PA6PBICN2** | 6 | 240 | 85 | 9'700 | 19'700 | 2.0 |
| **PA8PBICN2** | 8 | 272 | 92 | 11'100 | 22'500 | 1.9 |
| **PA10PBICN2** | 10 | 280 | 92 | 9'400 | 19'000 | 2.0 |
| **PA12PBICN2** | 12 | 270 | 85 | 15'500 | 32'000 | 2.0 |

A combination of $^1$H NMR spectroscopy, solid-state IR spectroscopy, and gel permeation chromatography (GPC), confirmed the chemical structures of the resulting polyamides (Figure 1, Table 1). However, their insolubility in common organic solvents required derivatization with trifluoroacetic anhydride (TFAA) to give the corresponding poly(trifluoroacetylimide)s. GPC could then be performed with HFIP as the eluent. The number average molecular weights ($M_n$) of 9'400 to 15'500 g/mol and the dispersities ($Đ$) of around 2.0 implied a degree of polymerization of between 13 and 20, indicative of a robust polycondensation procedure (Table 1).

The broad absorption at 2800–3300 $cm^{-1}$ in the solid-state infrared (IR) spectra of compound **5** can be assigned to the O–H stretching vibration, while the band at 1712 $cm^{-1}$ corresponds to the C=O stretching vibration of a free carboxylic acid group (Figure 1*a*). After polycondensation, these bands were replaced by a characteristic amide A (N–H stretching) absorption at 3302–3307 $cm^{-1}$ with a shoulder at around 3390 $cm^{-1}$ (Figure 1*b*), the amide I (C=O stretching) peak at 1631–1642 $cm^{-1}$, and the amide II band at 1537–1545 $cm^{-1}$, along with with C=O stretching bands and benzene C=C vibrations from the perylene bisimide core at 1703–1706, 1657–1664, and 1597–1600 $cm^{-1}$ (Figure 1*c*).[52] In each case, the maximum and the shoulder of the amide A peak were associated with hydrogen-bonded and free (non-hydrogen-bonded) amide groups, respectively. The peak position and its full width at half maximum (FWHM < 100 $cm^{-1}$) were similar to those observed in typical semicrystalline polyamides.[53]

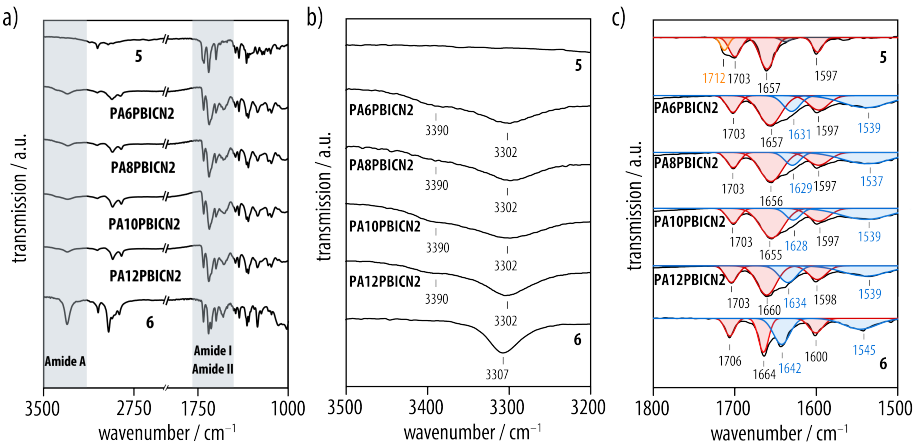


**Figure 1.** Solid-state IR spectra of the of the dicyanoperylene bisimide -containing polyamides **PA*n*PBICN2**. *a*) The formation of amide bonds was confirmed from comparison of the solid-state IR spectra of the polyamides **PA*n*PBICN2** with that of compounds **5** and **6**. *b*) The characteristic amide A *c*) and amide I and II bands (blue) appeared after polycondensation, along with the C=O stretching vibrations of the perylene bisimide core (red).

*Crystalline Morphology of the Polyamides*

Wide-angle X-ray diffraction (WAXD) patterns of the as-synthesized polyamides **PA*n*PBICN2** (*n* = 6, 8, 10, 12) powders showed clear Bragg peaks superimposed on an amorphous background, indicating the presence of an ordered phase in the solid-state, consistent with the IR spectroscopic data. Peaks were observed for all the materials at 2$\theta$ ranging from 42.0–43.1 ° (broad), 23.8–29.5 ° (strong), 18.2–19.9 ° (strong), 12.1–12.9 °, 10.3–10.5 °, and 3.7–4.5 ° (strong), corresponding to spacings of 2.1–2.2 Å, 3.0–3.7 Å, 4.5–4.9 Å, 6.9–7.3 Å, 8.4–8.6 Å and 19.5–23.5 Å (Figure 2*a*). This suggested the

increase in the length of the aliphatic segment ($n$) not to have a major qualitative influence on the crystalline morphology of the polyamides. However, the spacings associated with the lowest angle peak visible in the WAXD patterns increased from 19.5 to 23.5 Å with increasing $n$ (Figure 2*b*), suggesting a systematic increase in the long period of the unit-cell. Peak deconvolution followed by subtraction of the amorphous background suggested a crystallinity index, $\chi$, of 43–53%, which is similar to the degrees of crystallinity observed in other semiaromatic polyamides obtained with the same method (Figure 2*c*).[54,55] The lamellar long period ($L_p$) arising from the periodic stacking of alternating crystalline and amorphous lamellae was estimated from small-angle X-ray scattering (SAXS) measurements to be in the range of 19–22.5 nm (Figure 2*c*). Combining WAXD crystallinity indexes and SAXS long period, it therefore implied lamellar thicknesses of roughly 9.1 nm for $n$ = 6, 8.5 nm for $n$ = 8, 10.2 nm for $n$ = 10 and 11.9 nm for $n$ = 12, assuming a simple two phase model, which was between 4 and 5 times the spacings corresponding to the lowest angle WAXD peaks in each case.

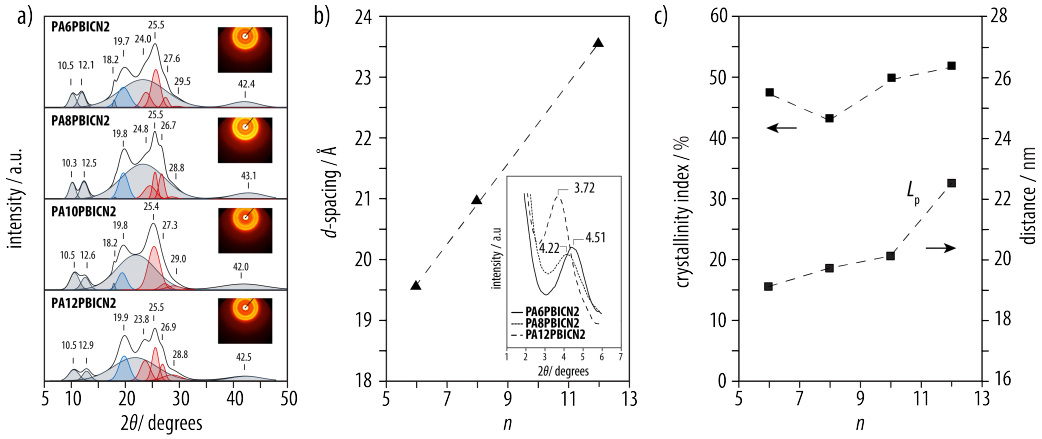


**Figure 2.** *a*) Wide angle X-Ray diffraction (WAXD) patterns of the as-synthesized **PA*n*PBICN2** ($n$ = 6, 8, 10, 12) powders were recorded at room temperature in transmission mode, along with the corresponding 2D patterns (insets). Deconvolution of these patterns was used to separate the amorphous background from the Bragg peaks. *b*) Systematic increase in the *d*-spacings corresponding to the lowest angle peaks in the WAXD patterns with increasing $n$ from 19.5 to 23.5 Å (inset: corresponding Bragg peaks). *c*) Estimated crystallity index as a function of $n$ based on the deconvolution of the WAXD patterns, together with the corresponding long period ($L_p$) estimated from small-angle X-ray scattering (SAXS) measurements.

Attemps to obtain a suitable single-crystal for WAXD analysis from model compound **6** from solution or by vacuum sublimation were unsuccessful. However, crystalline structures obtained for similar centrosymmetric **PBICN2** derivatives without amide groups, as well as our own UV-vis spectroscopic investigations (see below) suggest that the roughly planar perylene bisimide moieties should show

parallel-displaced π–π stacking with an interplanar distance of approximately 3.4 Å, consistent with the strong Bragg reflection at $2\theta$ = 25.4–25.5 ° observed in the present case, and the aliphatic groups in an extended conformation.[56–58] Moreover, in common with other polyamides derived from centrosymmetric aromatic diacids and linear aliphatic diamines with even *n*, **PA*n*PBICN2** (*n* = 6, 8, 10, 12) is expected to show a stable α-type crystalline phase in which fully extended aliphatic linkages form stacked planar hydrogen-bonded sheets.[10,44] At the same time, in order to maintain a reasonable packing density, the chain direction of the aliphatic linkages must be strongly tilted away from the planes of the more bulky perylene moieties.

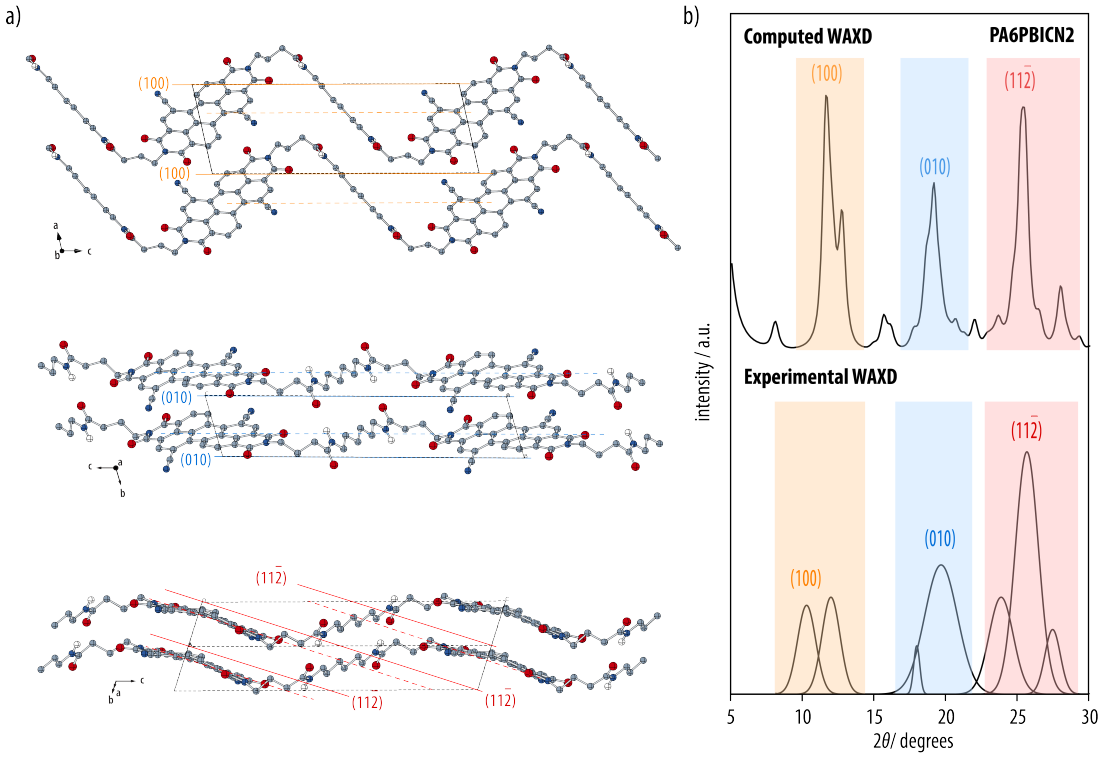


**Figure 3.** *a*) Model structure for **PA6PBICN2** assuming a triclinic unit cell with the *c*-axis parallel to the polymer backbone. *b*) Simulated WAXD powder pattern from the structure in *a*) in comparison with a fitting of the experimental WAXD peaks in Figure 2a.

A model triclinic unit cell for **PA6PBICN2** containing a single repeat unit was constructed on this basis and energy-minimized using the Dreiding II force-field and charge equilibration, resulting in unit cell parameters, $a$ = 8.37 Å, $b$ = 5.24 Å, $c$ = 23.08 Å, $\alpha$ = 102.55 °, $\beta$ = 96.4 °, and $\gamma$ = 112.65 °, and a relative density of 1.295 (Figure 3*a*). The planes of the perylene bisimide cores were twisted by about 15.6 ° in the relaxed structure, consistent with previously reported values for similar model compounds,[59] and their interplanar spacing was 3.4 Å. The intermolecular hydrogen bond angles and distances associated with the amide groups were N–H···O ∢ 169 ° and H···O $d$ = 2.2 Å, respectively. Simulated

WAXD powder patterns from this structure confirmed strong scattering at $2\theta$ of around 25 ° from the perylene stacks, whose planes were approximately parallel to $(11\bar{2})$ in this representation, a strong (010) peak at $2\theta \approx 19.2$ ° and significant additional scattering at lower angles from the (10*l*) planes, in reasonable qualitative agreement with the corresponding experimental WAXD patterns (Figure 3*b*), bearing in mind the significant 1,6-regioisomer content of the specimens. Indeed, while the experimental WAXD patterns did not permit unambiguous independent determination of the unit cell parameters, the diffraction peaks for **PA6PBICN2** could be indexed by analogy with the model structure, implying $a$ = 9.22 Å, $b$ = 5.00 Å, $c$ = 20.45 Å, $\alpha$ = 100.50 °, $\beta$ = 93.50 °, and $\gamma$ = 112.85 °, and a relative density of 1.37, suggesting stronger tilting of the chain direction of the aliphatic linkages away from the planes of the perylene moieties than in the model structure, and hence a reduced long period.

*Thermomechanical Properties of the Polyamides*

The thermal stability of the polyamides was investigated by thermogravimetric analysis (TGA) at a heating rate of 10 °C/min under a nitrogen atmosphere. All the polyamides **PA*n*PBICN2** ($n$ = 6, 8, 10, 12) as well as the monomer **5** and the model compound **6** exhibited a mass loss of 1–2 wt% at about 300 °C, defined as the onset of decomposition, followed by a strong increase in the rate of mass loss above 350 °C (Figure 4*a*, Supplementary Figure S3), as well as high residual mass due to carbonization of the peryelene bisimide units. Differential scanning calorimetry (DSC) indicated there to be no significant melting transition prior to the onset of degradation (Figure 4*b*).

Dynamic mechanical analysis (DMA) performed on powder specimens of **PA*n*PBICN2** ($n$ = 6, 8, 10, 12) at room temperature revealed a shear modulus in the range 0.75–0.93 GPa in each case, which is significantly higher than that of the fully aliphatic PA610 but lower than that of the commercially available engineering semiaromatic polyamide PA6TI (Figure 4*c*). Increasing the length of the aliphatic segment, $n$, is not expected to have a major effect on the resulting modulus, as the apparent crystallinities of the different polyamides **PA*n*PBICN2** ($n$ = 6, 8, 10, 12) as obtained by WAXD were similar (Figure 2*c*).

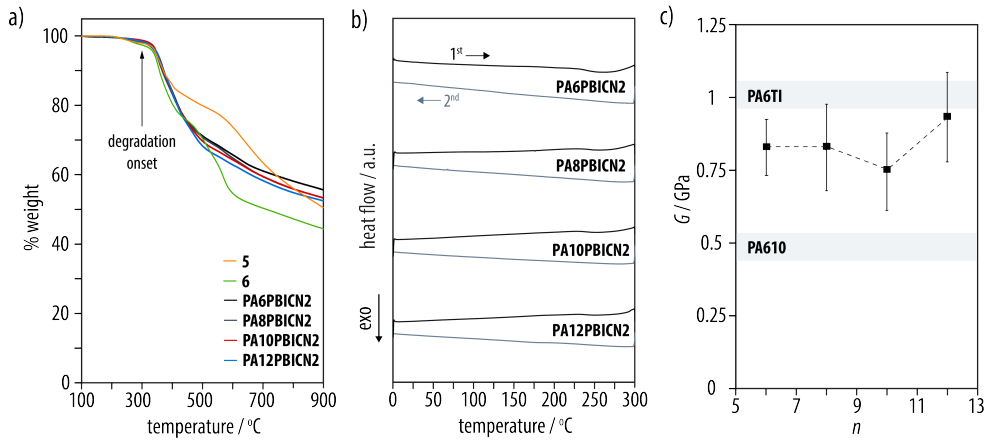


**Figure 4.** *a*) Thermogravimetric analysis (TGA) scans of **PA*n*PBICN2** (*n* = 6, 8, 10, 12) as well as **5** and **6** performed at heating rate of 10 °C/min under nitrogen atmosphere. *b*) Differential scanning calorimetry (DSC) heating and cooling runs of **PA*n*PBICN2** (*n* = 6, 8, 10, 12) confirmed the absence of any significant thermal transistions before the degradation onset temperature of 300 °C. *c*) The shear modulus, *G*, of **PA*n*PBICN2** as a function of *n* calculated from dynamic mechanical analysis measurements (shear mode, 1 Hz at room temperature). Representative values from the commercially available polyamides PA610 and PA6TI are shown for comparison.

*Optoelectronic Properties*

UV-vis absorption and fluorescence spectroscopy used to investigate the packing and the photophysical properties of the polyamide **PA6PBICN2** as a representative example and model compound **6** in solution and in the solid-state. Both **PA6PBICN2** and **6** showed a strong $S_0$–$S_1$ absorption in TFA ($c$ = $10^{-4}$ mol/L) at 527 nm (0–0) with higher energy vibronic bands at 492 (0–1) and 462 nm (0–2) (Figure 5*a,b*, solid black lines).[60] The ratio of the 0–0 and the 0–1 ($A_{0-0}/A_{0-1}$) absorption intensities was around 1.48, which is similar to typical values for perylene bisimide derivatives in solution and indicated spectroscopic aggregates to be absent in TFA at this concentration.[61–63] The weak absorption band at 391 nm was attributed to the $S_0$–$S_2$ transition of the perylene bisimide.[60] Emission spectra from dilute solutions of both **PA6PBICN2** and **6** in TFA ($c$ = $10^{-6}$ mol/L) revealed a Stokes shift of 15 nm and well-resolved vibronic fine structure patterns with fluorescence maxima at 542 nm and shoulders at 574 nm (Figure 5*a,b*, solid red lines) mirroring the corresponding absorption spectra.

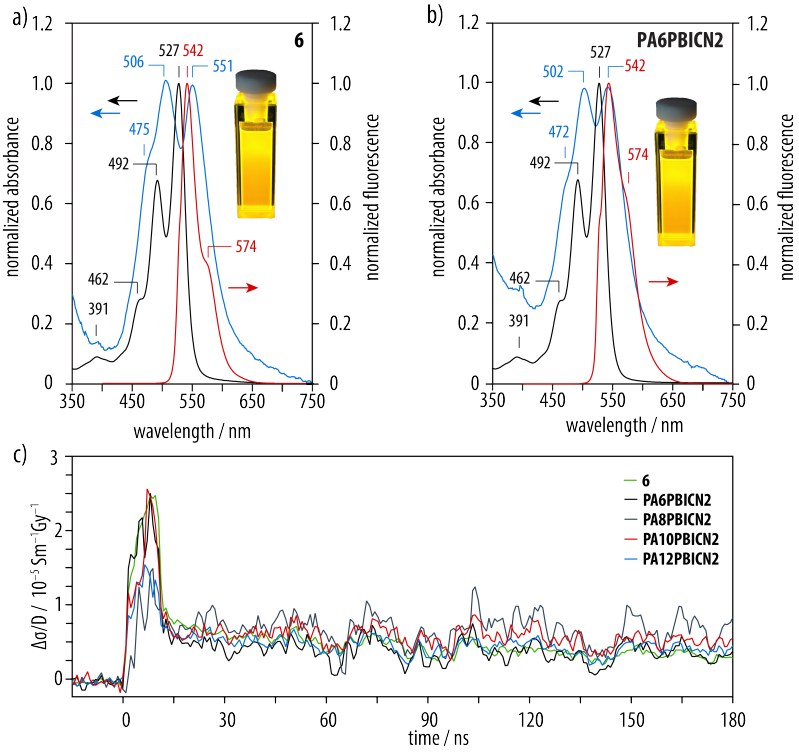


**Figure 5.** Normalized UV-vis (solution-phase and thin film) absorption and solution-phase fluorescence spectra of *a*) model compound **6** and *b*) **PA6PBICN2.** The solution-phase spectra were obtained from TFA solutions (black: absorption spectra, $c = 10^{-4}$ mol/L; red: fluorescence spectra $c = 10^{-6}$ mol/L), while thin film spectra were obtained from spin-coated thin films on quartz substrates (blue). The inset shows the corresponding specimens under UV light (254 nm). *c*) The change in conductivity on irradiation with a 10 ns electron pulse for **PA*n*PBICN2** (*n*= 6, 8, 10, 12) and model compound **6**, measured by time-resolved microwave conductivity.

Thin films prepared by spin coating of **PA6PBICN2** and **6** from TFA ($c = 10^{-3}$ mol/L) onto quartz substrates exhibited spectral signatures that were markedly different from the solution-phase spectra. The two main absorptions at 551 and 506 nm for **6**, and 542 and 522 nm for **PA6PBICN2**, as well as the shoulders at 472–475 nm could be assigned to the 0–0, 0–1, and 0–2 bands of the $S_0$–$S_1$ transitions, and a weak $S_0$–$S_2$ absorption was observed at 391 nm in both cases (Figure 5*a,b*, blue lines). The weak red-shift (15–20 nm) of the highest-wavelength absorptions, the strong decrease in the respective $A_{0-0}/A_{0-1}$ ratios to 0.98 for **6** and 1.0 for **PA6PBICN2**, and the almost complete quenching of fluorescence suggested pronounced H-type coupling of the dicyanoperylene bisimide chromophores, typical of an almost cofacial, parallel-displaced arrangement of these chromophores in the solid-state.[64–67]

Finally, in order to gain insight in the conductive properties of these materials, we then performed pulse-radiolysis time-resolved microwave conductivity (PR-TRMC) experiments on bulk specimens of **PA*n*PBICN2** (*n* = 6, 8, 10, 12) and the model compound **6,** as described above. The PR-TRMC

measurements resulted in clear conductivity transients, yielding one-dimensional charge carrier mobilities, $\mu_{1D}$ = 1.4 × $10^{-2}$ $cm^2 V^{-1} s^{-1}$ (**6**), 1.1 × $10^{-2}$ $cm^2 V^{-1} s^{-1}$ (**PA6PBCIN2**), 1.2 × $10^{-2}$ $cm^2 V^{-1} s^{-1}$ (**PA8PBCIN2**), 1.0 × $10^{-2}$ $cm^2 V^{-1} s^{-1}$ (**PA10PBCIN2**), and 1.0 × $10^{-2}$ $cm^2 V^{-1} s^{-1}$ (**PA12PBCIN2**) (Figure 5*c*). These values were comparable with those reported for other electron-conducting, bisubstituted perylene bisimides, including liquid-crystalline materials [68,69] and hydrogen-bonded perylene bisimide organogelators,[70] and about one order of magnitude higher than those of hole-conducting, hydrogen-bonded oligothiophene derivatives.[31,71]

## Conclusions

We used solution-phase polycondensation to prepare a series of novel polyamides containing dicyanoperylene bisimide repeat units, which showed morphologies and thermomechanical characteristics similar to existing semiaromatic polyamides. Based on IR and optical spectroscopy as well as molecular modelling and WAXD, we suggest the perylene bisimide units in the polyamides to form stacks with a parallel-displaced π–π arrangement. This arrangement gives rise to strong H-type coupling in the solid-state UV-vis spectra and is expected to provide percolation pathways for charge transport, as reflected by charge carrier mobilities of about 0.01 $cm^2 V^{-1} s^{-1}$, which is in the same range as for typical crystalline electron-conducting materials based on perylene bisimide derivatives. Our results hence demonstrate that the incorporation of cyanoperylene bisimide repeat units into a polyamide backbone may be used to prepare polymers that combine the charge transport properties of typical electron-deficient π-conjugated segments with thermomechanical properties characteristic of high-performance engineering polyamides.

## Acknowledgments

The authors gratefully acknowledge funding from the *Schweizerischer Nationalfonds* (SNF grants 200020–144417 and 200020–162774). The research leading to these results at Delft University of Technology has received funding from the European Research Council Horizon 2020 ERC Grant Agreement no. 648433.

## References


(1) Marchildon Keith. Polyamides – Still Strong After Seventy Years. *Macromol. React. Eng.* **2011**, *5* (1), 22–54.
(2) Zhang, C. Progress in Semicrystalline Heat-Resistant Polyamides. *E-Polym.* **2018**, *0* (0). https://doi.org/10.1515/epoly-2018-0094.
(3) Brady, M.; Brady, P. Technology Developments in Automotive Composites. *Reinf. Plast.* **2010**, *54* (6), 25–29.
(4) García, J. M.; García, F. C.; Serna, F.; de la Peña, J. L. High-Performance Aromatic Polyamides. *Prog. Polym. Sci.* **2010**, *35* (5), 623–686.
(5) Ahmed, D.; Hongpeng, Z.; Haijuan, K.; Jing, L.; Yu, M.; Muhuo, Y. Microstructural Developments of Poly (p-Phenylene Terephthalamide) Fibers during Heat Treatment Process: A Review. *Mater. Res.* **2014**, *17* (5), 1180–1200.
(6) García, J. M.; García, F. C.; Serna, F.; de la Peña, J. L. Aromatic Polyamides (Aramids). In *Handbook of Engineering and Specialty Thermoplastics*; Thomas, S., Visakh, P. M., Eds.; John Wiley & Sons, Inc.: Hoboken, NJ, USA, 2011; pp 141–181.
(7) Luo, K.; Wang, Y.; Yu, J.; Zhu, J.; Hu, Z. Semi-Bio-Based Aromatic Polyamides from 2,5-Furandicarboxylic Acid: Toward High-Performance Polymers from Renewable Resources. *RSC Adv.* **2016**, *6* (90), 87013–87020.
(8) Noriega, R.; Rivnay, J.; Vandewal, K.; Koch, F. P. V.; Stingelin, N.; Smith, P.; Toney, M. F.; Salleo, A. A General Relationship between Disorder, Aggregation and Charge Transport in Conjugated Polymers. *Nat. Mater.* **2013**, *12* (11), 1038–1044.
(9) Wang, S.; Fabiano, S.; Himmelberger, S.; Puzinas, S.; Crispin, X.; Salleo, A.; Berggren, M. Experimental Evidence That Short-Range Intermolecular Aggregation Is Sufficient for Efficient Charge Transport in Conjugated Polymers. *Proc. Natl. Acad. Sci.* **2015**, *112* (34), 10599–10604.
(10) Candau, N.; Galland, S.; Cretenoud, J.; Balog, S.; Michaud, V.; chenal, J.-M.; Lame, O.; Plummer, C. J. G.; Frauenrath, H. High-Performance Polyamides with Engineered Disorder Show Exceptional Ductility. *Be Submitt.*
(11) Lee, S. S.; Phillips, P. J. Melt Crystallized Polyamide 6.6 and Its Copolymers, Part I. Melting Point – Lamellar Thickness Relations in the Homopolymer. *Eur. Polym. J.* **2007**, *43* (5), 1933–1951.
(12) Root, S. E.; Savagatrup, S.; Printz, A. D.; Rodriquez, D.; Lipomi, D. J. Mechanical Properties of Organic Semiconductors for Stretchable, Highly Flexible, and Mechanically Robust Electronics. *Chem. Rev.* **2017**, *117* (9), 6467–6499.
(13) Heeger, A. J. Nobel Lecture: Semiconducting and Metallic Polymers: The Fourth Generation of Polymeric Materials. *Rev. Mod. Phys.* **2001**, *73* (3), 681–700. https://doi.org/10.1103/RevModPhys.73.681.
(14) Beaujuge, P. M.; Fréchet, J. M. J. Molecular Design and Ordering Effects in π-Functional Materials for Transistor and Solar Cell Applications. *J. Am. Chem. Soc.* **2011**, *133* (50), 20009–20029.
(15) Rahmanudin, A.; Sivula, K. Molecular Strategies for Morphology Control in Semiconducting Polymers for Optoelectronics. *Chim. Int. J. Chem.* **2017**, *71* (6), 369–375.
(16) Yang, Y.; Liu, Z.; Zhang, G.; Zhang, X.; Zhang, D. The Effects of Side Chains on the Charge Mobilities and Functionalities of Semiconducting Conjugated Polymers beyond Solubilities. *Adv. Mater.* **2019**, *31* (46), 1903104.
(17) Ocheje, M. U.; Charron, B. P.; Nyayachavadi, A.; Rondeau-Gagné, S. Stretchable Electronics: Recent Progress in the Preparation of Stretchable and Self-Healing Semiconducting Conjugated Polymers. *Flex. Print. Electron.* **2017**, *2* (4), 043002.
(18) Rahmanudin, A.; Yao, L.; Sivula, K. Conjugation Break Spacers and Flexible Linkers as Tools to Engineer the Properties of Semiconducting Polymers. *Polym. J.* **2018**, *50* (8), 725–736.
(19) Mei, J.; Bao, Z. Side Chain Engineering in Solution-Processable Conjugated Polymers. *Chem. Mater.* **2014**, *26* (1), 604–615. https://doi.org/10.1021/cm4020805.
(20) Marty, R.; Szilluweit, R.; Sánchez-Ferrer, A.; Bolisetty, S.; Adamcik, J.; Mezzenga, R.; Spitzner, E.-C.; Feifer, M.; Steinmann, S. N.; Corminboeuf, C.; Frauenrath, H. Hierarchically Structured Microfibers of "Single Stack" Perylene Bisimide and Quaterthiophene Nanowires. *ACS Nano* **2013**, *7* (10), 8498–8508.
(21) Tian, L.; Szilluweit, R.; Marty, R.; Bertschi, L.; Zerson, M.; Spitzner, E.-C.; Magerle, R.; Frauenrath, H. Development of a Robust Supramolecular Method to Prepare Well-Defined Nanofibrils from Conjugated Molecules. *Chem. Sci.* **2012**, *3* (5), 1512–1521.
(22) Hafner, R. J.; Tian, L.; Brauer, J. C.; Schmaltz, T.; Sienkiewicz, A.; Balog, S.; Flauraud, V.; Brugger, J.; Frauenrath, H. Unusually Long-Lived Photocharges in Helical Organic Semiconductor Nanostructures. *ACS Nano* **2018**, *12* (9), 9116–9125.
(23) Marty, R.; Nigon, R.; Leite, D.; Frauenrath, H. Two-Fold Odd–Even Effect in Self-Assembled Nanowires from Oligopeptide-Polymer-Substituted Perylene Bisimides. *J. Am. Chem. Soc.* **2014**, *136* (10), 3919–3927.
(24) Stone, D. A.; Hsu, L.; Stupp, S. I. Self-Assembling Quinquethiophene–Oligopeptide Hydrogelators. *Soft Matter* **2009**, *5* (10), 1990–1993.
(25) Wall, B. D.; Diegelmann, S. R.; Zhang, S.; Dawidczyk, T. J.; Wilson, W. L.; Katz, H. E.; Mao, H.-Q.; Tovar, J. D. Aligned Macroscopic Domains of Optoelectronic Nanostructures Prepared via Shear-Flow Assembly of Peptide Hydrogels. *Adv. Mater.* **2011**, *23* (43), 5009–5014.
(26) Besar, K.; Ardoña, H. A. M.; Tovar, J. D.; Katz, H. E. Demonstration of Hole Transport and Voltage Equilibration in Self-Assembled π-Conjugated Peptide Nanostructures Using Field-Effect Transistor Architectures. *ACS Nano* **2015**, *9* (12), 12401–12409.
(27) Ardoña, H. A. M.; Tovar, J. D. Peptide π-Electron Conjugates: Organic Electronics for Biology? *Bioconjug. Chem.* **2015**, *26* (12), 2290–2302. https://doi.org/10.1021/acs.bioconjchem.5b00497.
(28) Hafner, R. J.; Görl, D.; Sienkiewicz, A.; Balog, S.; Frauenrath, H. Long-Lived Photocharges in Supramoelcular Polymers of Low-Bandgap Chromophores. *Chem. – Eur. J.* **2020**, chem.201904561.
(29) Rep, D. B. A.; Roelfsema, R.; van Esch, J. H.; Schoonbeek, F. S.; Kellogg, R. M.; Feringa, B. L.; Palstra, T. T. M.; Klapwijk, T. M. Self-Assembly of Low-Dimensional Arrays of Thiophene Oligomers from Solution on Solid Substrates. *Adv. Mater.* **2000**, *12* (8), 563–566.

(30) Würthner, F.; Bauer, C.; Stepanenko, V.; Yagai, S. A Black Perylene Bisimide Super Gelator with an Unexpected J-Type Absorption Band. *Adv. Mater.* **2008**, *20* (9), 1695–1698.
(31) Pratihar, P.; Ghosh, S.; Stepanenko, V.; Patwardhan, S.; Grozema, F. C.; Siebbeles, L. D. A.; Würthner, F. Self-Assembly and Semiconductivity of an Oligothiophene Supergelator. *Beilstein J. Org. Chem.* **2010**, *6*, 1070–1078.
(32) Würthner, F.; Thalacker, C.; Sautter, A.; Schärtl, W.; Ibach, W.; Hollricher, O. Hierarchical Self-Organization of Perylene Bisimide–Melamine Assemblies to Fluorescent Mesoscopic Superstructures. *Chem. – Eur. J.* **2000**, *6* (21), 3871–3886.
(33) Özen, B.; Tirani, F. F.; Scopelliti, R.; Frauenrath, H. Structure-Property Relationships in Bithiophenes with Hydrogen-Bonded Substituents. *submitted*
(34) Gebers, J.; Özen, B.; Hartmann, L.; Schaer, M.; Suárez, S.; Bugnon, P.; Scopelliti, R.; Steinrück, H.-G.; Konovalov, O.; Magerl, A.; Brinkmann, M.; Petraglia, R.; de Silva, P.; Corminboeuf, C.; Frauenrath, H. Crystallization and OFET Performance of a Hydrogen-Bonded Quaterthiophene. *Chem. – Eur. J.* **2020**. https://doi.org/10.1002/chem.201904562.
(35) Murthy N. Sanjeeva. Hydrogen Bonding, Mobility, and Structural Transitions in Aliphatic Polyamides. *J. Polym. Sci. Part B Polym. Phys.* **2006**, *44* (13), 1763–1782.
(36) Yao, J.; Yu, C.; Liu, Z.; Luo, H.; Yang, Y.; Zhang, G.; Zhang, D. Significant Improvement of Semiconducting Performance of the Diketopyrrolopyrrole–Quaterthiophene Conjugated Polymer through Side-Chain Engineering via Hydrogen-Bonding. *J. Am. Chem. Soc.* **2016**, *138* (1), 173–185.
(37) Ocheje, M. U.; Charron, B. P.; Cheng, Y.-H.; Chuang, C.-H.; Soldera, A.; Chiu, Y.-C.; Rondeau-Gagné, S. Amide-Containing Alkyl Chains in Conjugated Polymers: Effect on Self-Assembly and Electronic Properties. *Macromolecules* **2018**, *51* (4), 1336–1344.
(38) Charron, B. P.; Ocheje, M. U.; Selivanova, M.; Hendsbee, A. D.; Li, Y.; Rondeau-Gagné, S. Electronic Properties of Isoindigo-Based Conjugated Polymers Bearing Urea-Containing and Linear Alkyl Side Chains. *J. Mater. Chem. C* **2018**, *6* (44), 12070–12078.
(39) Lin, Y.-C.; Shih, C.-C.; Chiang, Y.-C.; Chen, C.-K.; Chen, W.-C. Intrinsically Stretchable Isoindigo–Bithiophene Conjugated Copolymers Using Poly(Acrylate Amide) Side Chains for Organic Field-Effect Transistors. *Polym. Chem.* **2019**, *10* (38), 5172–5183.
(40) Ocheje, M. U.; Selivanova, M.; Zhang, S.; Van Nguyen, T. H.; Charron, B. P.; Chuang, C.-H.; Cheng, Y.-H.; Billet, B.; Noori, S.; Chiu, Y.-C.; Gu, X.; Rondeau-Gagné, S. Influence of Amide-Containing Side Chains on the Mechanical Properties of Diketopyrrolopyrrole-Based Polymers. *Polym. Chem.* **2018**, *9* (46), 5531–5542.
(41) Oh, J. Y.; Rondeau-Gagné, S.; Chiu, Y.-C.; Chortos, A.; Lissel, F.; Wang, G.-J. N.; Schroeder, B. C.; Kurosawa, T.; Lopez, J.; Katsumata, T.; Xu, J.; Zhu, C.; Gu, X.; Bae, W.-G.; Kim, Y.; Jin, L.; Chung, J. W.; Tok, J. B.-H.; Bao, Z. Intrinsically Stretchable and Healable Semiconducting Polymer for Organic Transistors. *Nature* **2016**, *539* (7629), 411–415.
(42) Muguruma, H.; Yudasaka, M.; Hotta, S. Vapor Polymerization Deposition of New Polyamide Thin Films Having Oligothiophene Segments in the Main Chain. *Thin Solid Films* **1999**, *339*, 120–122.
(43) Muguruma, H.; Matsumura, K.; Hotta, S. Molecular Orientation of Oligothiophene-Based Polyamide Thin Films Fabricated by Vapor Deposition Polymerization. *Thin Solid Films* **2002**, *405*, 77–80.
(44) Özen, B.; Candau, N.; Temiz, C.; Grozema, F. C.; Fadaei Tirani, F.; Scopelliti, R.; Chenal, J.-M.; Plummer, C. J. G.; Frauenrath, H. Engineering Polymers with Improved Charge Transport Properties from Bithiophene-Containing Polyamides. *J. Mater. Chem. C* **2020**, https://doi.org/10.1039/C9TC06544J.
(45) Gebers Jan; Rolland Damien; Marty Roman; Suàrez Stéphane; Cervini Luca; Scopelliti Rosario; Brauer Jan Cornelius; Frauenrath Holger. Solubility and Crystallizability: Facile Access to Functionalized Π-Conjugated Compounds with Chlorendylimide Protecting Groups. *Chem. – Eur. J.* **2014**, *21* (4), 1542–1553.
(46) Würthner, F.; Stepanenko, V.; Chen, Z.; Saha-Möller, C. R.; Kocher, N.; Stalke, D. Preparation and Characterization of Regioisomerically Pure 1,7-Disubstituted Perylene Bisimide Dyes. *J. Org. Chem.* **2004**, *69* (23), 7933–7939.
(47) Mayo, S. L.; Olafson, B. D.; Goddard, W. A. DREIDING: A Generic Force Field for Molecular Simulations. *J. Phys. Chem.* **1990**, *94* (26), 8897–8909.
(48) Infelta, P. P.; de Haas, M. P.; Warman, J. M. The Study of the Transient Conductivity of Pulse Irradiated Dielectric Liquids on a Nanosecond Timescale Using Microwaves. *Radiat. Phys. Chem. 1977* **1977**, *10* (5), 353–365.
(49) Warman, J. M.; de Haas, M. P.; Dicker, G.; Grozema, F. C.; Piris, J.; Debije, M. G. Charge Mobilities in Organic Semiconducting Materials Determined by Pulse-Radiolysis Time-Resolved Microwave Conductivity: π-Bond-Conjugated Polymers versus π −π-Stacked Discotics. *Chem. Mater.* **2004**, *16* (23), 4600–4609.
(50) Yamazaki, N.; Higashi, F.; Kawabata, J. Studies on Reactions of the N-Phosphonium Salts of Pyridines. XI. Preparation of Polypeptides and Polyamides by Means of Triaryl Phosphites in Pyridine. *J. Polym. Sci. Polym. Chem. Ed.* **1974**, *12* (9), 2149–2154.
(51) Cretenoud, J.; Özen, B.; Schmaltz, T.; Görl, D.; Fabrizio, A.; Corminboeuf, C.; Tirani, F. F.; Scopelliti, R.; Frauenrath, H. Synthesis and Characterization of Semiaromatic Polyamides Comprising Benzofurobenzofuran Repeating Units. *Polym. Chem.* **2017**, *8* (14), 2197–2209.
(52) Akers, K.; Aroca, R.; Hort, A. M.; Loutfy, R. O. Molecular Organization in Perylene Tetracarboxylic Di-Imide Solid Films. *Spectrochim. Acta Part Ldots* **1988**, *44A*, 1129–1135.
(53) Skrovanek, D. J.; Painter, P. C.; Coleman, M. M. Hydrogen Bonding in Polymers. 2. Infrared Temperature Studies of Nylon 11. *Macromolecules* **1986**, *19*, 699–705.
(54) Li, M.; Dingemans, T. J. Synthesis and Characterization of Semi-Crystalline Poly(Decamethylene Terephthalamide) Thermosets. *Polymer* **2017**, *108*, 372–382.
(55) Guan, X. Crystallization of Polyamide 66 Copolymers at High Supercoolings. *PhD Thesis Univ. Tenn. Knoxv.* **2004**, 284.
(56) Liscio, F.; Milita, S.; Albonetti, C.; D'Angelo, P.; Guagliardi, A.; Masciocchi, N.; Della Valle, R. G.; Venuti, E.; Brillante, A.; Biscarini, F. Structure and Morphology of PDI8-CN2 for n-Type Thin-Film Transistors. *Adv. Funct. Mater.* **2012**, *22* (5), 943–953.
(57) Rivnay, J.; Jimison, L. H.; Northrup, J. E.; Toney, M. F.; Noriega, R.; Lu, S.; Marks, T. J.; Facchetti, A.; Salleo, A. Large Modulation of Carrier Transport by Grain-Boundary Molecular Packing and Microstructure in Organic Thin Films. *Nat. Mater.* **2009**, *8* (12), 952–958.

(58) Hädicke, E.; Graser, F. Structures of Three Perylene-3,4,9,10-Bis(Dicarboximide) Pigments. *Acta Crystallogr. Sect. C* **1986**, *42* (2), 195–198.
(59) Delgado, M. C. R.; Kim, E.-G.; Filho, D. A. da S.; Bredas, J.-L. Tuning the Charge-Transport Parameters of Perylene Diimide Single Crystals via End and/or Core Functionalization: A Density Functional Theory Investigation. *J. Am. Chem. Soc.* **2010**, *132* (10), 3375–3387.
(60) Jiménez, Á. J.; Lin, M.-J.; Burschka, C.; Becker, J.; Settels, V.; Engels, B.; Würthner, F. Structure–Property Relationships for 1,7-Diphenoxy-Perylene Bisimides in Solution and in the Solid State. *Chem Sci* **2014**, *5* (2), 608–619.
(61) Yagai, S.; Usui, M.; Seki, T.; Murayama, H.; Kikkawa, Y.; Uemura, S.; Karatsu, T.; Kitamura, A.; Asano, A.; Seki, S. Supramolecularly Engineered Perylene Bisimide Assemblies Exhibiting Thermal Transition from Columnar to Multilamellar Structures. *J. Am. Chem. Soc.* **2012**, *134* (18), 7983–7994.
(62) Giaimo, J. M.; Lockard, J. V.; Sinks, L. E.; Scott, A. M.; Wilson, T. M.; Wasielewski, M. R. Excited Singlet States of Covalently Bound, Cofacial Dimers and Trimers of Perylene-3,4:9,10-Bis(Dicarboximide)s. *J. Phys. Chem. A* **2008**, *112* (11), 2322–2330.
(63) Kaufmann, C.; Bialas, D.; Stolte, M.; Würthner, F. Discrete π-Stacks of Perylene Bisimide Dyes within Folda-Dimers: Insight into Long- and Short-Range Exciton Coupling. *J. Am. Chem. Soc.* **2018**, *140* (31), 9986–9995. https://doi.org/10/gd5s46.
(64) Spano, F. C. The Spectral Signatures of Frenkel Polarons in H- and J-Aggregates. *Acc. Chem. Res.* **2010**, *43* (3), 429–439. https://doi.org/10.1021/ar900233v.
(65) Würthner, F.; Chen, Z.; Dehm, V.; Stepanenko, V. One-Dimensional Luminescent Nanoaggregates of Perylene Bisimides. *Chem. Commun.* **2006**, No. 11, 1188. https://doi.org/10.1039/b517020f.
(66) Dehm, V.; Chen, Z.; Baumeister, U.; Prins, P.; Siebbeles, L. D. A.; Würthner, F. Helical Growth of Semiconducting Columnar Dye Assemblies Based on Chiral Perylene Bisimides. *Org. Lett.* **2007**, *9* (6), 1085–1088. https://doi.org/10.1021/ol0700963.
(67) Seibt, J.; Marquetand, P.; Engel, V.; Chen, Z.; Dehm, V.; Würthner, F. On the Geometry Dependence of Molecular Dimer Spectra with an Application to Aggregates of Perylene Bisimide. *Chem. Phys.* **2006**, *328* (1–3), 354–362.
(68) Chen, Z.; Debije, M. G.; Debaerdemaeker, T.; Osswald, P.; Würthner, F. Tetrachloro-Substituted Perylene Bisimide Dyes as Promising n-Type Organic Semiconductors: Studies on Structural, Electrochemical and Charge Transport Properties. *ChemPhysChem* **2004**, *5* (1), 137–140. https://doi.org/10.1002/cphc.200300882.
(69) Debije, M. G.; Chen, Z.; Piris, J.; Neder, R. B.; Watson, M. M.; Müllen, K.; Würthner, F. Dramatic Increase in Charge Carrier Lifetime in a Liquid Crystalline Perylene Bisimide Derivative upon Bay Substitution with Chlorine. *J Mater Chem* **2005**, *15* (12), 1270–1276. https://doi.org/10.1039/B416407E.
(70) Li, X.-Q.; Stepanenko, V.; Chen, Z.; Prins, P.; Siebbeles, L. D. A.; Würthner, F. Functional Organogels from Highly Efficient Organogelator Based on Perylene Bisimide Semiconductor. *Chem Commun* **2006**, No. 37, 3871–3873. https://doi.org/10.1039/B611422A.
(71) Schoonbeek, F. S.; van Esch, J. H.; Wegewijs, B.; Rep, D. B. A.; de Haas, M. P.; Klapwijk, T. M.; Kellogg, R. M.; Feringa, B. L. Efficient Intermolecular Charge Transport in Self-Assembled Fibers of Mono- and Bithiophene Bisurea Compounds. *Angew. Chem. Int. Ed.* **1999**, *38* (10), 1393–1397.

## Table of Contents Figure